ELSEVIER

Biophysical Chemistry 63 (1997) 107–118

Biophysical Chemistry

Binding of phosphate and sulfate anions by purine nucleoside phosphorylase from *E. coli*: ligand-dependent quenching of enzyme intrinsic fluorescence

Borys Kierdaszuk [a,*], Anna Modrak-Wójcik [a], David Shugar [a,b]

[a] *University of Warsaw, Institute of Experimental Physics, Department of Biophysics, 93 Zwirki i Wigury Street, 02089 Warsaw, Poland*
[b] *Institute of Biochemistry and Biophysics, Polish Academy of Sciences, 5[a] Pawinskiego Street, 02106 Warsaw, Poland*

Received 26 April 1996; revised 20 August 1996; accepted 9 September 1996

Abstract

Steady-state and time-resolved emission spectroscopy was applied to a study of the binary and ternary complexes of pure *E. coli* purine nucleoside phosphorylase (PNP) with phosphate (P_i; a substrate) and a close non-substrate analogue (sulfate; SA). The quenching of enzyme fluorescence by P_i was bimodal, best described by two modified Stern–Volmer equations fitted independently for "low" (below 0.5 mM P_i) and "high" (above 0.5 mM P_i) ligand concentrations. At $P_i > 0.5$ mM, binding is characterized by a fortyfold higher dissociation constant ($K_{d2} = 1.12 \pm 0.10$ mM), i.e. by a lower affinity for phosphate, with a sevenfold lower quenching constant and 1.6-fold higher accessibility. By contrast, the binding of SA, and the resultant fluorescence quenching, was unimodal, with $K_d = 1.36 \pm 0.07$ mM, comparable to the K_d for P_i at "high" P_i, with a total binding capacity of one sulfate or phosphate group per enzyme subunit. SA proved to be a competitive inhibitor of phosphorolysis with $K_i = 1.2 \pm 0.2$ mM vs. P_i, hence similar to its K_d. SA at a concentration of 5 mM did not affect the P_i affinity at $P_i < 0.5$ mM, but led to a reduced affinity and twofold higher P_i binding capacities at $P_i > 0.5$ mM. The resultant fluorescence quenching by P_i decreased at 5 mM SA, with lower Stern–Volmer constant (K_{SV}) and fractional accessibility (f_a) values. Increasing concentrations of P_i reduced the enzyme affinity for SA, characterized by a higher K_d. The Hill model showed negative cooperative binding of P_i in the absence and presence of 5 mM SA with Hill coefficients $h = 0.60 \pm 0.01$ and $h = 0.83 \pm 0.07$, respectively. SA exhibited non-cooperative binding in the absence of P_i ($h = 1.08 \pm 0.01$) and negative cooperative binding in the presence of P_i ($h < 1$). PNP fluorescence decays were best fitted to a sum of two exponentials, with an average lifetime of 2.40 ± 0.14 ns, unchanged on interaction with quenching ligands, and pointing to static quenching. The overall results are relevant to the properties of PNP from various sources, in particular to the design of potent bisubstrate analogue inhibitors.

Keywords: Purine nucleoside phosphorylase; Protein fluorescence; Anion binding; Fluorescence quenching; Time-resolved fluorescence

Abbreviations: PNP, purine nucleoside phosphorylase; Ino, inosine; Guo, guanosine; m^7Guo, 7-methylguanosine; P_i, orthophosphate; SA, sulfate ion; FPLC, fast protein liquid chromatography; SDS, sodium dodecyl sulfate; PAGE, polyacrylamide gel electrophoresis; TCSPC, time-correlated single-photon counting

* Corresponding author. Fax.: (+4822)-220248; e-mail: borys@asp.biogeo.uw.edu.pl

PII S0301-4622(96)02239-9

1. Introduction

The ubiquitous purine nucleoside phosphorylase (PNP; purine nucleoside:orthophosphate ribosyl transferase, EC 2.4.2.1.), a key enzyme of the anabolic and catabolic pathways of purine nucleosides, catalyzes the reversible cleavage of the glycosidic bond of ribo- and 2′-deoxyribonucleosides of guanine and hypoxanthine in higher organisms, as well as of adenine in some prokaryotes, e.g. *E. coli* and *S. typhimurium*, as follows:

$$\beta - \text{nucleoside} + P_i \rightleftarrows \text{purinebase} + \alpha - D - \text{pentose} - 1 - \text{phosphate}$$

Since the report of Giblett et al. [1], PNP is recognized as a primary target for the chemotherapeutic treatment of child lymphopenia associated with a complete lack of PNP activity. Such symptoms suggest several chemotherapeutic applications of PNP inhibitors. They are considered to be promising potential immunosuppressive agents [2,3] for suppressing the host versus graft reaction in organ transplantation, for the treatment of T-cell mediated autoimmune diseases such as lupus or rheumatoid arthritis [4,5], and in the therapy of T-cell leukemias, without affecting humoral resistance. PNP inhibitors are also promising drugs for the prevention of intracellular phosphorolytic cleavage of therapeutically active nucleoside analogues. It is therefore not surprising that widespread attention is directed to studies on the mechanism of the action of this enzyme from various sources and to searches for more potent inhibitors [5–8].

The enzyme from a variety of eukaryotes is a trimer [5], whereas that from prokaryotes is a hexamer [9,10]. The native form of *E. coli* PNP is a hexamer with an M_r of 138 kDa [9] and a subunit M_r of 24 kDa [9,10], further confirmed by sequencing [11]. Although the *E. coli* enzyme was crystallized long ago [12], its three-dimensional structure has not been determined.

Crystal structures have been reported for the enzyme from human erythrocytes [13] and for a complex of the calf spleen enzyme with an acyclonucleoside inhibitor [14] at resolutions of 2.75 Å and 2.9 Å, respectively. However, the human erythrocyte enzyme was crystallized from ammonium sulfate, so that all phosphate-binding sites are blocked by sulfate. By contrast, the calf spleen enzyme was crystallized from polyethylene glycol, with the phosphate-binding sites free. The resulting structure, when resolved, may be expected to reveal how sulfate ions (SA) affect the structure of the human enzyme, the more so in that the sequences of the two enzymes display a high degree of homology [15]. The effects of these two ions on the structures of various proteins have been recently reviewed [16–18].

Particularly interesting is the influence of the concentration of P_i on the affinity of the enzyme for inhibitors, especially bisubstrate analogue inhibitors which simultaneously interact with the binding sites for nucleosides and phosphate [19,20]. The K_i values for such inhibitors are markedly dependent on the P_i concentration, frequently being most effective at the low mM P_i concentrations prevailing in human cells [21,22].

The substrate/inhibitor properties of PNP with respect to P_i and other ions has received much less attention than nucleoside substrates and nucleoside analogue inhibitors. The substrate properties of arsenate have been reported [9,23,24]. Several phosphonates have also been described as substrates of calf spleen PNP [25], but we have been unable to confirm this for the purified enzyme from either calf spleen or *E. coli* (unpublished). Also, no data are yet extant on ion inhibitors of the enzyme.

Furthermore, the kinetics of the enzyme from various sources are rather complex and exhibit biphasic saturation curves with P_i as substrate [5,26,27], typical for substrate-induced negative cooperativity. This phenomenon has been described as the ability of a ligand binding at one site on a macromolecule to influence ligand binding at a different site on the same macromolecule [28]. We herein describe the use of fluorescent emission techniques to studies on the interaction of P_i and its close non-substrate analogue sulfate with *E. coli* PNP. The *E. coli* enzyme was selected for the initial studies following our ability to purify it to homogeneity. It is relatively stable, has no isovariants [10], and differs considerably from its mammalian counterparts and other bacterial strains with regard to substrate specificity [29].

2. Experimental

2.1. Materials and methods

Inosine (Ino), *N*(7)-methylguanosine (m^7Guo), ammonium sulfate (SA; grade III; P_i content less than 5 ppm), mono- and dibasic sodium phosphates and KCl (ACS grade), and xanthine oxidase (grade III; 1 U mg^{-1}) were products of Sigma Chemical Co. (St. Louis, MO, USA). Tris was obtained from Merck (Darmstadt, GFR), L-tyrosine was from Aldrich (Steinheim, GFR), and electrophoretic reagents were from Bio-Rad (Richmond, VA., USA). All solutions were prepared with high-quality MilliQ water. All other reagents and materials were of the highest quality commercially available, and only those of spectral grade, checked by UV absorption and/or fluorescence emission, were employed.

Ultraviolet absorption was monitored with a Kontron (Switzerland) UVIKON 930 recording instrument fitted with a thermostatically controlled cell compartment, using 5 and 10 mm pathlength cuvettes.

Measurements of the pH (± 0.05) were carried out with a Jenway (UK) pH-meter equipped with a combination semimicro electrode and temperature sensor.

Protein concentrations were determined by the Lowry method with human serum albumin as standard [30], and/or from absorbance measurements with $\varepsilon_{1\%}^{278} = 2.7$ [31].

Enzyme activity was monitored at 25°C in 50 mM phosphate buffer (pH 7.0), spectrophotometrically by the coupled xanthine oxidase procedure with Ino as substrate [32], and/or directly spectrophotometrically by following the changes in absorption of m^7Guo at 260 nm ($\Delta\varepsilon = 4.6 \times 10^3$) as substrate [33].

2.2. Enzyme purification

Partially purified PNP from *E. coli* (about 60% pure, approximately 60 U mg^{-1}), a gift from Dr. G. Koszalka (Wellcome Research Laboratories, Research Triangle Park, NC, USA) was further purified by affinity chromatography on Sepharose 6B activated by Formycin B, as described by Schrader et al. [34] for Sepharose 6B activated by adenosine. The enzyme sample (around 1 mg of protein per millilitre) in 50 mM Tris–HCl buffer (pH 7.6) containing 1 mM β-mercaptoethanol (buffer A) was applied at a flow rate of 0.20 ml min^{-1} to the affinity column (16 cm × 2 cm) equilibrated with the same buffer. The column was washed with 150 ml of buffer A, followed by 150 ml of 100 mM Tris–HCl buffer (pH 8.0) containing 0.5 M NaCl and 1 mM β-mercaptoethanol. The enzyme was eluted with 50 mM phosphate buffer (pH 7.6) containing 4 mM Ino and 1 mM β-mercaptoethanol, and 4 ml fractions were collected every 30 min. Ultrafiltration on a Centricon-30 concentrator (Amicon Inc., MA, USA) was used to remove the products of phosphorolysis, as well as to concentrate the enzyme samples. This resulted in almost twofold purification. However, the product was still unsuitable for fluorescence measurements inasmuch as it included contaminant proteins (less than 5%) with weak bands at 18 ± 2 and 45 ± 4 kD on SDS-PAGE [35], also observed previously by Hall and Krenitsky [10].

The enzyme was then subjected to gel filtration chromatography by FPLC on a Superose™ 12,HR 10/30 (300 ± 10 mm) column with a 280 nm UV-1 detector (Pharmacia LKB Biotechnology, Sweden). The column was equilibrated, elution was carried out at a flow rate of 0.4 ml min^{-1}, with 50 mM Tris–HCl buffer (pH 7.6) containing 0.1 M KCl, and 0.2 ml fractions were collected. PNP eluted as a single symmetric band with a constant ratio of absorbancy to enzyme activity, and SDS-PAGE exhibited a single polypeptide band, visualized by positive image silver staining [36]. The purified enzyme had a specific activity of 105 U mg^{-1}, similar to earlier results [37]. Analytical gel filtration chromatography, with molecular weight markers (size 1, Boehringer Manheim, GFR: β-amylase, $M_r = 200\,000$; BSA, $M_r = 67\,000$; carbonic anhydrase, $M_r = 29\,000$; cytochrome C, $M_r = 12\,400$) gave a native M_r of 134 ± 14 kD. SDS-PAGE led to a subunit M_r of 23 ± 2 kD, consistent with earlier results [9,10,38].

2.3. Steady-state fluorescence measurements

Steady-state fluorescence spectra were monitored at 25°C on a Spex (USA) Fluoromax spectrofluorimeter with 4 nm spectral resolution for excitation and emission. Protein samples (1–2.5 μM) were

prepared in 370–380 μl of 50 mM Tris–HCl (pH 7.6) in 5 × 5 mm Suprasil cuvettes.

Such solutions still contained background contaminant phosphate, 1 μM, estimated spectrophotometrically [39]. As will be seen below, this was sufficiently low as not to affect overall results and conclusions. We therefore refer to these solutions as controls free from P_i, unless otherwise stated.

Protein fluorescence was excited at several wavelengths in the range 260–290 nm, and fluorescence spectra were recorded in the range 290–400 nm. For quenching studies, additions to the enzyme were made from quencher stock solutions prepared in the same buffer and at the same pH as the enzyme sample, and changes in fluorescence were usually monitored at 300 and 320 nm (with $\lambda_{exc} = 280$ nm), and at 310 and 320 nm (with $\lambda_{exc} = 265$ nm). Emission and excitation spectra were recorded prior to and after titration. Dilution did not exceed 12%, and fluorescence intensity was corrected for the dilution factor. Background emission (below 5%) was eliminated by subtracting the signal from buffer containing the appropriate quantity of ligand. The total absorbance of the enzyme sample did not exceed 0.1 at 278 nm, to eliminate inner-filter effects. The specific activity of the enzyme was not affected by titration, as checked by activity measurements before and after the experiments.

2.4. Analysis of steady-state fluorescence quenching data

Three types of quenching mechanisms were considered in analyses of fluorescence quenching data: dynamic quenching, due to time-dependent diffusion-controlled collisions between fluorophore and quencher; static quenching, resulting from the formation of a non-fluorescent ground state complex between fluorophore and quencher; and combined dynamic and/or static quenching of fluorophores differing in accessibility to the quencher. Each mechanism may be described by a Stern–Volmer type equation [40] which relates the relative decrease of enzyme fluorescence (F_0/F) to the concentration of the quenching ligand, $[L_0]$.

For dynamic quenching

$$F_0/F = \tau_0/\tau = 1 + K_{SV}[L_0] \qquad (1)$$

where F and F_0 are the fluorescence intensities in the presence and absence of a quenching ligand, τ_0 and τ are the fluorescence lifetimes in the absence and presence of a quencher, and K_{SV} is the Stern–Volmer constant for dynamic quenching, equal to $k_q\tau_0$, where k_q is the bimolecular rate constant for the quenching process. The Stern–Volmer constant K_{SV} is a measure of the propensity to quenching of the excited state(s) of the fluorophores. Hence a plot of F_0/F or τ_0/τ against $[L_0]$ should be linear for a homogeneous population of emitting fluorophores, when all are equally accessible to the quenching ligand and are subject only to dynamic quenching [41]. For static quenching $\tau_0/\tau = 1$ and K_{SV} is then the static quenching constant, equal to the association constant for the enzyme–ligand complex [40].

Numerical fitting analysis (see below) revealed that Eq. (1) and (2) did not fit the experimental points. Hence, a modified form of the Stern–Volmer equation was used to analyze the quenching of heterogeneous emitting fluorophores [42,43]

$$F_0/(F_0 - F) = 1/([L_0]f_aK_{SV}) + 1/f_a \qquad (2)$$

where K_{SV} is the Stern–Volmer constant and f_a is the fractional accessibility, i.e. the fraction of protein fluorescence (tyrosine residues) accessible to the quencher. A plot of $F_0/(F_0 - F)$ vs. $1/[L_0]$ should yield a straight line with a slope of $1/(f_aK_{SV})$ and an intercept of $1/f_a$. The magnitude of f_a is subject to two interpretations: (a) as the relative number of fluorophore residues accessible to the quencher; or (b) as the fractional fluorescence quenched by direct interaction accompanying conformational changes of the macromolecule. An unequivocal interpretation must await determination of the three-dimensional structure of the enzyme.

2.5. Ligand binding

To obtain the dissociation constants (K_d) for each binding site and the binding capacity (N) for the ligand on each enzyme subunit, data analyses were performed in the form of Scatchard plots [44]

$$V/[L] = (N - V)/K_d \qquad (3)$$

where V is the number of moles of ligand bound per mole of total enzyme subunits, $[L] = [L_0] - [E_0](F_0 - F)/(F_0 - F_i)$ is the molar concentration of free

ligand, $[L_0]$ is the total concentration of ligand, $[E_0]$ is the total concentration of enzyme subunits, and F_i is the fluorescence of the enzyme sample at saturating ligand concentrations. Ligand-binding analyses were based on the assumption of a linear relationship between the fluorescence of the free enzyme or enzyme–ligand complex and the enzyme or enzyme–ligand concentration, respectively. This led to $V = (F_0 - F)/(F_0 - F_i)$ [45].

Alternatively, Eq. (3) may be transformed as follows [46]

$$\nu = N[L]/(K_d + [L]) \quad (4)$$

and for two classes of binding sites (states) of the enzyme characterized by different dissociation constants (K_{d1}, K_{d2}) and binding capacities (N_1, N_2)

$$V = N_1[L]/(K_{d1} + [L]) + N_2[L]/(K_{d1} + [L]) \quad (5)$$

Ligand-binding data were also analyzed according to the Hill equation in the logarithmic form (Eq. (6)), and the Hill coefficient (h) and apparent dissociation constant (K_d^{app}) used as a measure of cooperative binding [47], as follows

$$\log[V/(1 - V)] = h \log[L_0] - \log K_d^{app} \quad (6)$$

The Eq. (1)–(6) were transformed to the function $F = f([L])$, and fitted using non-linear regression analysis. The χ^2 values and residuals — the differences, and/or relative differences, between calculated and experimental values — were used to test the quality of the fits.

2.6. Time-resolved fluorescence measurements

Time-correlated single-photon counting (TCSPC) measurements of fluorescence [48,49] were performed on an IBH time-resolved spectrofluorimeter (IBH Consultants Ltd., UK) equipped with a high-frequency flash lamp and two excitation and emission monochromators operated at 4 nm spectral resolution. Fluorescence excited by the vertical polarized pulse was collected by a Suprasil lens and passed through a monochromator and a Glan-Thompson polarizer set at the magic angle (54.7°). The fluorescence signal, free from polarization effects, was given directly by the magic angle signal, after the subtraction of background fluorescence.

The fluorescence decay data were fitted to sums of one, two and/or three exponentials (Eq. (7)), convoluted with the instrument response, by a least-squares fitting procedure [49], using IBH software (IBH Consultants Ltd, Glasgow, UK)

$$I(t) = \sum_i \alpha_i \exp(-t/\tau_i) \quad (7)$$

where α_i are the amplitudes associated with the decay time τ_i. The fractional intensity decay f_i is given by $f_i = \alpha_i\tau_i/\sum_j \alpha_j\tau_j$ and the mean decay time $\langle\tau\rangle = \sum_i f_i\tau_i$. The quality of fit was evaluated by the structure observed in residuals plots and by the reduced χ_R^2 values. The overall resolution of the IBH system was 200 ps and permitted a satisfactory fit of the sum of two exponentials.

Fluorescence decay measurements were also performed at the Center for Fluorescence Spectroscopy (University of Maryland, Baltimore, USA) on a system equipped with a Rhodamine 6G dye laser, which was synchronously pumped by an Nd–Yag laser, mode-locked, cavity-dumped (8 MHz) and tuned to 570 nm, and frequency-doubled to 285 nm for efficient excitation of the tyrosine residues of PNP. The dye laser pulse full width at half maximum (FWHM) was about 5 ps at a repetition rate of 3.795 MHz. The detection system was based on a Hamamatsu microchannel plate photomultiplier set up in the TCSPC mode. The overall response time of the laser system was 70 ps FWHM. High-resolution fluorescence decays of the enzyme in the absence and presence of P_i (data not shown) permitted a good fit of the sum of three exponantial terms, and confirmed the results obtained with the IBH system.

3. Results

3.1. Fluorescence characteristics of E. coli PNP; effect of quenching ions

Fluorescence spectra of pure PNP were recorded in 50 mM Tris–HCl buffer (pH 7.6) at 25°C in the absence and presence of phosphate and sulfate. In the absence of quenching ligands, the emission maximum was located at 304 nm and the excitation maximum at 276 nm (Fig. 1), typical for tyrosine-containing proteins [50], and quite different from the emission of the analogous enzymes from mammalian

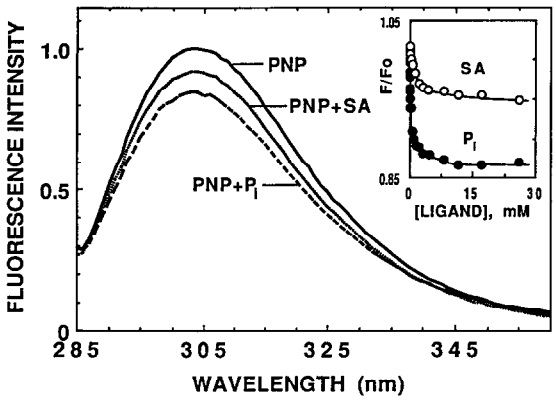

Fig. 1. Fluorescence spectra (λ_{exc} = 280 nm) of PNP from *E. coli* in 50 mM Tris–HCl buffer (pH 7.6) and at (————) 1 μM (background) and (---) 100 mM (saturated) concentration of P_i, and at (· · ·) 100 mM (saturated) concentration of SA. The insert shows the effect of (●) P_i and (○) SA concentration on the relative fluorescence intensity (F/F_0) at 300 nm with λ_{exc} = 280 nm.

sources (calf spleen and human erythrocytes), dominated by tryptophan emission [51]. The addition of ions was accompanied by partial quenching of the enzyme fluorescence (Fig. 1, insert) with no effect on the location of the excitation and emission maxima (Fig. 1). This was not due to an effect of increasing ionic strength, since the addition of 100 mM KCl did not affect the enzyme fluorescence or the enzyme activity.

The typical tyrosine-like emission spectrum of *E. coli* PNP is consistent with its known content of six tyrosine residues and no tryptophan [11]. Its sensitivity to interaction with P_i and SA, with a quenching pattern independent of excitation and emission wavelengths, suggests a single common quenching process for all six tyrosine residues (but see below). Hence the steady-state titration of emission as a function of ion concentration, together with time-resolved spectra, should permit the characterization of protein–ion interactions.

3.2. Enzyme fluorescence quenching by phosphate binding

The Stern–Volmer plot for fluorescence quenching by P_i (Fig. 2A) was not linear, and non-linear regression analysis revealed that the Stern–Volmer equation (Eq. (1) in Section 2.5) for dynamic and static quenching did not fit the experimental points. Furthermore, we could not obtain a good fit to the modified Stern–Volmer Eq. (2) for the entire range of fluorescence quenching by P_i (Fig. 2B) with any single set of parameters (K_{SV}, f_a). Hence, fluorescence quenching was described by two processes

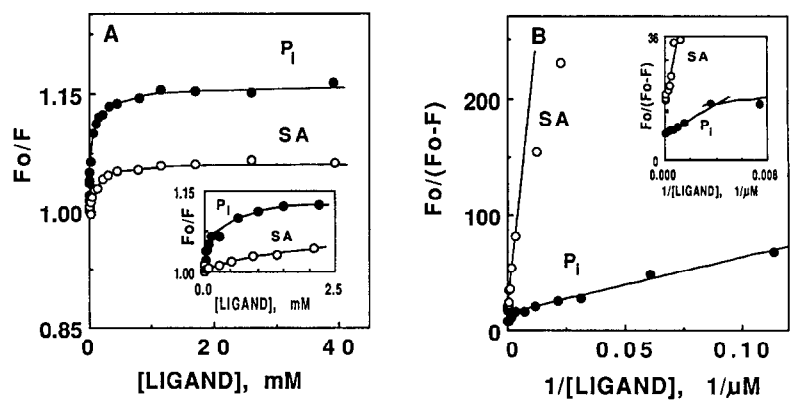

Fig. 2. Steady-state quenching of PNP fluorescence at 300 nm (λ_{exc} = 280 nm) by (•) P_i and (○) SA. (A) Stern–Volmer plot of enzyme fluorescence (expressed as the fraction of unquenched fluorescence, F_0) as a function of ligand concentration. (B) Modified Stern–Volmer plot of the decrease of fluorescence ($F_0 - F$) (expressed as the fraction of the unquenched fluorescence F_0) as a function of the reciprocal ligand concentration. The inserts show the same data at the low (A) and high (B) concentration range of the ligands. The solid lines represent the Stern–Volmer equation fitted for the entire concentration range of SA, or independently for the high and low concentration ranges of P_i.

Table 1
Stern–Volmer constants (K_{SV}, f_a) obtained from fits of the modified Stern–Volmer Eq. (3) to enzyme fluorescence quenching data [a]

Quenching ligand	Ligand present during titration	Ligand concn. range (μM)	K_{SV} (μM^{-1})	f_a
P_i	SA, 0 mM	5–280	0.019 ± 0.001	0.112 ± 0.004
		1000–11000	0.0028 ± 0.0001	0.182 ± 0.007
	SA, 5 mM	40–100	0.0076 ± 0.0021	0.0231 ± 0.0004
		1500–17000	0.00027 ± 0.00002	0.114 ± 0.006
SA	P_i, 1 μM	130–17000	0.00070 ± 0.00004	0.075 ± 0.003
	P_i, 25 μM	300–17000	0.00075 ± 0.00006	0.045 ± 0.003
	P_i, 75 μM	300–17000	0.00053 ± 0.00038	0.015 ± 0.001

[a] The titration was performed at 25°C in 50 mM Tris–HCl buffer (pH 7.6) as described in Section 2.3. For phosphate, due to the poor fits of one modified Stern–Volmer Eq. (2) to the entire range of fluorescence quenching, two such equations were fitted independently for the two ranges of ligand concentration, as indicated.

with different quenching constants and different accessibilities to the quencher. Two ranges of fluorescence quenching data, denoted as "strong" and "weak" quenching, were analyzed separately and the results of the best fits are presented in Table 1. A transition between the two ranges of quenching was observed at about 0.5 mM P_i (Fig. 2B). For "high" P_i (above 0.5 mM), the quenching constant was about sevenfold lower, and the accessibility was 1.6-fold higher, than for "low" P_i (below 0.5 mM), where $K_{SV} = 0.019 \pm 0.001$ and $f_a = 0.112 \pm 0.004$.

The results of enzyme–P_i binding, calculated from the fluorimetric titration of enzyme with P_i, are shown as a non-linear Scatchard plot in Fig. 3. Non-linear regression fitting of different models of ligand binding, e.g. with one, two or three classes of binding sites (or states of the enzyme), gave a best fit with two classes of binding sites (or two-state model, Eq. (5)), shown in Table 2. There is apparently a "high affinity" state of the enzyme with a dissociation constant $K_{d1} = 29.4 \pm 2.2$ μM and a binding capacity $N_1 = 0.48 \pm 0.01$ of phosphate molecules per subunit of hexameric enzyme, and a "low affinity" state with an approximately thirtyfold higher dissociation constant (K_{d2}) and with a binding capacity $N_2 = 0.54 \pm 0.01$ (Table 2). The maximum binding capacity of both forms of the enzyme is consequently one phosphate anion per 23 kDa subunit of the native enzyme (see Section 2.2), as previously proposed by Jensen [27].

3.3. Enzyme fluorescence quenching by sulfate binding

The propensity of the sulfate anion to compete with P_i in binding to human PNP is best illustrated by the fact that, in the three-dimensional structure of this enzyme crystallized from ammonium sulfate, all the phosphate-binding sites are occupied by sulfate anion [13]. This prompted us to examine SA activity vs. *E. coli* PNP in the presence and absence of P_i.

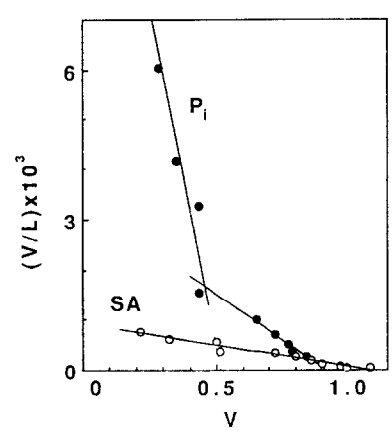

Fig. 3. Experimental data from Fig. 2 expressed in the form of Scatchard plots for the binding of (•) P_i and (◦) SA by *E. coli* PNP: the number of moles of bound P_i (or SA) per mole of enzyme subunit and per molar concentration of free P_i (or SA) ($V/[L]$) are expressed as a function of the number of moles of bound P_i (or SA) per mole of enzyme subunit (V).

Table 2
Dissociation constants (K_{d1}, K_{d2}) and relative binding capacities (N_1, N_2) obtained from fits of a two-state model (Eq. (5)) for the binding of P_i, and of a one-state model (Eq. (4)) for the binding of SA, with *E. coli* PNP in 50 mM Tris–HCl buffer (pH 7.6). Also shown are the Hill constants (h) and apparent dissociation constants (K_d^{app}) obtained from fits of the Hill model (Eq. (6)) to the same data

Quenching ligand	Ligand present during titration	N_1	K_{d1} (μM)	N_2	K_{d2} (mM)	h	K_d^{app} (mM)
P_i	SA 0 mM	0.48 ± 0.01	29.4 ± 2.2	0.54 ± 0.01	1.12 + 0.10	0.60 ± 0.01	0.027 ± 0.002
	5 mM	0.08 ± 0.02	27.7 ± 1.1	1.03 ± 0.03	3.94 + 0.10	0.83 ± 0.07	0.31 ± 0.16
SA	P_i 1 μM	–	–	1.01 ± 0.01	1.36 ± 0.07	1.08 ± 0.01	1.21 ± 0.09
	25 μM	–	–	1.00 ± 0.02	1.76 ± 0.21	0.79 ± 0.03	1.37 ± 0.13
	75 μM	–	–	1.02 ± 0.01	2.81 ± 0.37	0.85 ± 0.07	1.07 ± 0.37

Enzyme activity was monitored spectrophotometrically [33] by following the changes in absorption of 200 μM m^7Guo as substrate at 260 nm ($\Delta\varepsilon = 4.6 \times 10^3$) in 50 mM Tris–HCl buffer (pH 7.0) containing 68, 81 and 93 μM of phosphate buffer (pH 7.0), at 37°C. The inhibition constant was calculated using the initial rate method. Initial rates were determined from linear regression fitting to at least 10 experimental points with an accuracy of 5% or less. The equation describing the competitive model of inhibition, $v = V_{max}/[(K_m/[P])(1 + [SA]/K_i) + 1]$, was fitted to the initial rates (v) measured at five concentrations of sulfate [SA] for each phosphate concentration [P_i], and apparent values of K_i calculated. The sulfate anion was not a substrate, but was a competitive inhibitor of phosphorolysis with $K_i = 1.2 \pm 0.2$ mM, confirmed by a Dixon plot of $1/v$ vs. [SA] (Fig. 4). Competition between SA and P_i was additionally confirmed by a plot of $[P_i]/v$ vs. [SA] giving the expected parallel linear plots (data not shown). These data indicate that SA and P_i compete for the same binding sites of *E. coli* PNP in the presence of a nucleoside substrate.

Unimodal fluorescence quenching was observed with SA (Fig. 2, bottom) in the absence of P_i, and good fits were obtained with a model of one set of emitter(s) described by one Eq. (2) in the concentration range 0.15–17 mM (Table 1). SA is a much weaker quencher than P_i at "high" concentration, characterized by a fourfold lower Stern–Volmer constant ($K_{SV} = 0.00070 \pm 0.00004$ μM^{-1}) and a 2.5-fold lower fractional accessibility ($f_a = 0.075 \pm 0.003$).

The results of enzyme–SA binding, calculated from the fluorimetric titration of enzyme with SA, are shown as a linear Scatchard plot in Fig. 3. Non-linear regression fitting of different models of ligand binding, e.g. with one, two or three classes of binding sites or states of the enzyme (for a discussion, see below), gave a best fit with one class of binding sites (or one-state model, Eq. (4)) for sulfate binding (Table 2) with a total binding capacity of one SA anion per enzyme subunit and a dissociation constant $K_d = 1.36 \pm 0.07$ mM, similar to that for P_i binding at "high" P_i concentrations ($K_{d2} = 1.12 \pm 0.10$ mM).

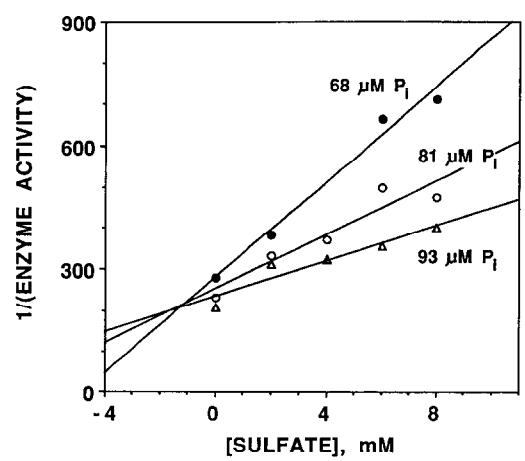

Fig. 4. Dixon plot for the inhibition of phosphorolysis of 200 μM m^7Guo by SA with *E. coli* PNP at pH 7 and 25°C. •, 68 μM P_i; ○, 81 μM P_i; Δ, 93 μM P_i. The solid lines represent linear equations fitted independently using the linear regression method (enzyme activity in arbitrary units).

3.4. Interaction between phosphate and sulfate binding

In the presence of 5 mM SA, quenching by P_i (Fig. 5, Table 1) was characterized by a 2.5-fold lower K_{SV} and a fivefold lower f_a for "low" P_i concentrations, and tenfold and 1.6-fold lower K_{SV} and f_a for "high" P_i concentrations. The P_i affinity at $P_i < 0.5$ mM was not affected by SA, while 5 mM SA led to a decreased affinity of P_i at $P_i > 0.5$ mM resulting in a 3.5-fold higher K_{d2} (3.94 ± 0.10 mM), and fivefold lower N_1 (0.08 ± 0.02) and twofold higher N_2 (1.03 ± 0.03) binding capacities of P_i at $P_i < 0.5$ mM and $P_i > 0.5$ mM, respectively.

With increasing P_i concentration, SA quenching of PNP fluorescence (Fig. 5, Table 1) remained unimodal, and was very weak at 75 μM P_i (Fig. 5), with a drastic decrease in SA binding (Table 2). Hence there is the same binding site for SA with a much lower fractional accessibility and Stern–Volmer constant (Table 1). The Stern–Volmer constant in the presence of 25 and 75 μM P_i was unchanged, but the accessibility of the binding site to SA decreased by 40% and 80%, respectively (Table 1). At 1 μM P_i, non-cooperative binding of SA (Fig. 6) occurs with a Hill coefficient $h = 1.08 \pm 0.01$. Increasing concentrations of P_i led to negative cooperative binding with Hill coefficients $h < 1$, and 1.3- and twofold higher dissociation constants at 25 and 75 μM P_i (Table 2). Furthermore, the Hill model revealed negative cooperative binding of P_i in the absence and presence of 5 mM SA, characterized by Hill coefficients $h < 1$, i.e. 0.60 ± 0.01 and 0.83 ± 0.01, respectively, and an elevenfold higher apparent dissociation constant ($K_d^{app} = 0.31 \pm 0.16$ mM) at 5 mM SA (Table 2).

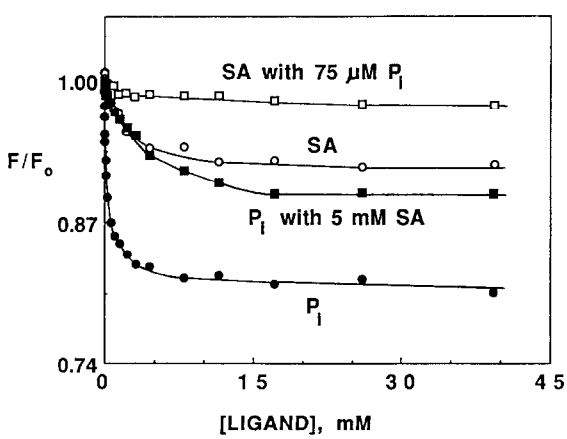

Fig. 5. Effect of SA on P_i quenching (and vice versa) of *E. coli* PNP fluorescence expressed as the relative decrease of enzyme fluorescence measured at different concentrations of P_i and/or SA.

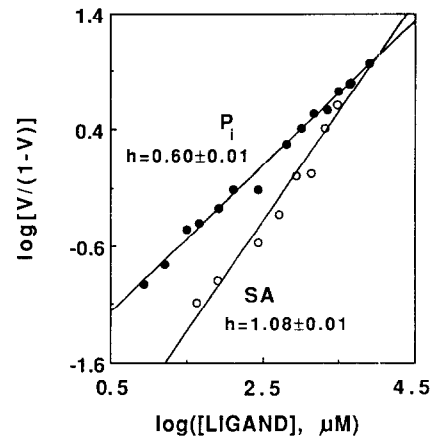

Fig. 6. Experimental data from Fig. 3 expressed in the form of Hill plots for the binding of (•) P_i and (○) SA by *E. coli* PNP: the number of moles of bound P_i (or SA) per mole of enzyme subunit (V) are expressed as a function of the concentration of P_i (or SA).

The negative cooperativity of the enzyme reflects the incomplete accessibility of the binding sites, dependent on the concentration of P_i. For $P_i < 0.5$ mM, binding of P_i occurs with high affinity, while the binding sites exhibit a so-called half-site reactivity, referred to as the binding capacity, $N_1 = 0.48 \pm 0.01$. For $P_i > 0.5$ mM, there is a decrease in the affinity of P_i, characterized by a fortyfold higher dissociation of the enzyme–P_i complex.

The quenching effects of phosphate and sulfate may be due to direct interactions with tyrosine residues, or indirectly by changes in the conformation of the protein with accompanying modifications in the vicinity of other tyrosine residues. Bearing in mind that *E. coli* PNP contains six tyrosine residues [11], the fractional fluorescence quenched at saturating concentrations of ligands corresponds roughly to one residue, the fluorescence of which is fully quenched by such interaction. The absence of an effect of complex formation on the mean fluorescence lifetime (see below) points to complex forma-

tion in the ground state, so that the Stern–Volmer constants may be considered as association constants of the complexes.

3.5. Time-resolved fluorescence of E. coli PNP and its complex with phosphate and sulfate

Experimental data for the fluorescence decay of PNP at 25°C in 50 mM Tris–HCl (pH 7.6), in the absence and presence of P_i and SA, were fitted with the sum of varying numbers of exponentials (Eq. (7) in Section 2.6) and a non-linear least-squares fitting procedure. The quality of the fits was evaluated by structures observed in residuals plots and by the reduced χ^2_R values.

The decays of PNP fluorescence were non-exponential both in the absence and presence of ligands, and required a sum of two exponential terms for good fits over a range of 10 ns. The results obtained from the fits (Table 3) show that interaction with P_i and SA affected only slightly the fractional intensities ($f_1 = 0.145(\pm 30\%)$, $f_2 = 0.855(\pm 5\%)$) and lifetimes ($\tau_1 = 0.6(\pm 30\%)$ ns, $\tau_2 = 2.7(\pm 5\%)$ ns) of the exponential components, with no effect on the average lifetime ($\langle\tau\rangle = 2.4(\pm 6\%)$ ns), so that interactions with P_i and SA leads uniquely to static quenching [40]. These results, further confirmed by high-resolution fluorescence decay data obtained on the TPSC system at the Center for Fluorescence Spectroscopy (University of Maryland, BA, USA), are consistent with the model for the static interaction of enzyme and ligand derived from measurements of this interaction on the intrinsic fluorescence of the enzyme (Sections 2.4 and 2.5).

Table 3
Multiexponential analysis of PNP fluorescence intensity decay at $\lambda_{exc} = 285 \pm 4$ nm (P_i) or 270 ± 4 nm (SA) and $\lambda_{em} = 320 \pm 4$ nm (P_i) or 310 ± 4 nm (SA)

Ligand added	Ligand concn. (mM)	α_i	f_i [a]	τ_i (ns)	$\langle\tau\rangle$ [b] (ns)	χ^2_R 1exp	χ^2_R 2exp
Phosphate	0 [c]	0.034	0.18	1.08	–	–	–
		0.061	0.82	2.77	2.47	1.25	1.00
	0.03	0.061	0.15	0.48	–	–	–
		0.067	0.85	2.66	2.35	1.53	1.12
	1.1	0.084	0.17	0.40	–	–	–
		0.065	0.83	2.62	2.25	1.36	0.87
	26.0	0.034	0.16	0.72	–	–	–
		0.048	0.84	2.64	2.33	1.30	0.94
Sulfate	0 [c]	0.014	0.12	0.55	–	–	–
		0.021	0.88	2.77	2.50	2.56	1.01
	61.0	0.016	0.11	0.45	–	–	–
		0.021	0.89	2.70	2.45	2.50	1.03

Measurements were performed at 25°C in 50 mM Tris–HCl (pH 7.6) containing phosphate buffer (pH 7.6) (P_i) or ammonium sulfate (SA) at different concentrations, as indicated.
[a] $f_i = \alpha_i\tau_i / \Sigma_j \alpha_j \tau_j$.
[b] $\langle\tau\rangle = \Sigma_i f_i \tau_i$.
[c] Actually 1 μM background (contaminant) concentration.

4. Discussion

The present findings are relevant to the properties of PNP in in vitro studies, where the concentration dependence of the negative cooperativity of phosphate binding reflects the negative cooperativity of enzyme kinetics [27]. They also point to the regulatory role of phosphate on the intracellular function of PNP, bearing in mind that cellular concentrations of P_i vary from about 1 mM in human erythrocytes to 3 mM for human lymphocytes and 5 mM for mouse cells [21,22].

By analogy with structural models for some other enzymes, e.g. hexokinase [52] and deoxycytidine kinase [45], the results of this study suggest that *E. coli* PNP can adopt (at least) two different states (or conformations) with high and low affinity for phosphate anions, respectively. With increasing phosphate concentration, the enzyme is shifted from the high to the low affinity state, characterized by an almost fortyfold-higher dissociation constant. By contrast, the sulfate anion, which competes with phosphate for a binding site of the latter, binds the low affinity state of the enzyme with a dissociation constant (1.36 ± 0.07 mM) similar to its apparent inhibition constant (1.2 ± 0.2 mM) for phosphorolysis via competition with P_i.

The affinity, albeit lower, of sulfate for phosphate binding sites is consistent with that observed for many other proteins [16]. A similar situation prevails for PNP from mammmalian sources, best illustrated by the fact that in human erythrocyte PNP crystallized from ammonium sulfate, all the phosphate-binding sites are fully occupied by sulfate anions [13]. In all probability, SA will also inhibit the mam-

malian enzymes by competition with P_i, and it would be of interest to determine the inhibition constant for this reaction.

The existence of two states of the enzyme with such different affinities for phosphate is obviously relevant to the kinetics of the enzyme as a function of the P_i concentration in the incubation medium. We refer here to one aspect, of key importance in the development of effective inhibitors. It was initially shown by Tuttle and Krenitsky [53] that, whereas the antiviral acyclonucleoside acyclovir is a moderate inhibitor of human erythrocyte PNP, independent of the P_i concentration in the medium, acyclovir diphosphate (but not monophosphate or triphosphate) is a highly potent inhibitor [53,54], with a K_i value at 1 mM P_i of 10 nM. In the presence of 50 mM P_i, the K_i for the inhibition of phosphorolysis is 500 nM [54]. It is of interest that the fiftyfold difference in K_i values is comparable to the fortyfold difference in affinity of the *E. coli* enzyme for P_i at low and high phosphate concentrations. The low K_i of acyclovir diphosphate in the presence of a low P_i concentration suggested that this compound occupies both the phosphate and nucleoside binding sites, i.e. behaves as a bisubstrate analogue inhibitor, the spacing between the purine base and the terminal phosphate being optimal for diphosphate (but not for the monophosphate or triphosphate), a result supported by X-ray diffraction data for a complex of the human enzyme with acyclovir diphosphate [55]. Hence, in effect, the terminal phosphate of acyclovir diphosphate effectively competes for the phosphate binding site of the enzyme at low P_i, where it is in the high affinity state.

The foregoing has stimulated the synthesis of other potential bisubstrate analogue inhibitors [19,20,56]. One such series comprises 9-(difluorophosphonoalkyl)guanines, which displayed potent activity versus PNP from human erythrocytes, calf spleen and what was referred to as *E. coli* [20]. However, the "*E. coli*" enzyme employed was a product of Sigma, referred to in the Sigma catalogue as "bacterial" PNP. We have elsewhere shown unequivocally that this enzyme, for which Sigma has refused to divulge the source, is not the *E. coli* enzyme [29]. Bearing in mind the differences in amino acid sequences between the mammalian enzymes [14,57] and that from *E. coli* [11], and the marked differences in substrate specificity between the two classes of enzymes [29], it is clearly desirable to examine the possibile inhibitory effects of these bisubstrate analogue inhibitors versus the highly purified *E. coli* enzyme, and such studies are now under way in our laboratories.

Acknowledgements

We are very much indebted to Dr. George Koszalka (Wellcome Research Laboratories, Research Triangle Park, NC, USA) for the generous gift of partially purified *E. coli* PNP, to Professor Joseph R. Lakowicz for making available facilities at the Center for Fluorescence Spectroscopy (University of Maryland, Baltimore, USA) for some time-resolved fluorescence measurements, to Dr. Agnieszka Bzowska for help in preparation of the affinity column (supported by KBN grant no. 6P04A06209) and to Mrs. Lucyna Magnowska for technical assistance. A. M.-W. is indebted for a doctoral grant from KBN (6P20303207). This work was supported by an International Research Scholars Award from the Howard Hughes Medical Institute (grant no. HHMI 75195-543401) and in part by grants no. 415149101, 6P20304605 and UM-141 from the Committee for Scientific Research (KBN, Poland). We are also indebted to the Polish Science Foundation (BIMOL Program) for purchase of some equipment.

References

[1] E.R. Giblett, A.J. Ammann, D.W. Wara, R. Sandman, and L.K. Diamond, Lancet, 1 (1975) 1010.
[2] R.B. Gilbertsen and J.C. Sircar, in C. Hansch, P.G. Sammes and J.B. Taylor (Eds.), Comprehensive Medicinal Chemistry, Vol. 2, Pergamon Press, Oxford, 1990, pp. 443–480.
[3] R.B. Gilbertsen, M.E. Scott, M.K. Dong, L.M. Kossarek, M.K. Bennett, D.J. Schrier and J.C. Sicar, Agents Actions, 22 (1987) 379.
[4] J.D. Stoeckler, C. Cambor, F.W. Burgess, S.B. Erban and R.E. Parks, Jr., Pharmacologist, 22 (1980) 99.
[5] J.D. Stoeckler, in R.I. Glazer, (Ed.), Developments in Cancer Chemotherapy, CRC Press, Boca Raton, FL, 1984, pp. 35–60.
[6] A. Bzowska, E. Kulikowska, D. Shugar, Chen Bing-Yi, B. Lindborg and N.G. Johansson, Biochem. Pharmacol., 41 (1991) 1791.
[7] J.A. Secrist, III, S. Niwas, J.D. Rose, Y.S. Babu, C.E. Bugg,

M.D. Erion, W.C. Guida, S.E. Ealick and J.A. Montgomery, J. Med. Chem., 36 (1993) 1847.
[8] J.A. Montgomery, S. Niwas, J.D. Rose, J.A. Secrist, III, Y.S. Babu, C.E. Bugg, M.D. Erion, W.C. Guida and S.E. Ealick, J. Med. Chem., 36 (1993) 55.
[9] K.F. Jensen and P. Nygaard, Eur. J. Biochem., 51 (1975) 253.
[10] W.W. Hall and T.A. Krenitsky, Prep. Biochem., 20 (1990) 75.
[11] M.S. Hershfield, S. Chaffee, L. Koro-Johnson, A. Mary, A.A. Smith and S.A. Short, Proc. Natl. Acad. Sci. U.S.A., 88 (1991) 7185.
[12] W.J. Cook, S.E. Ealick, T.A. Krenitsky, J.D. Stoeckler, J.R. Helliwell and C.E. Bugg, J. Biol. Chem., 260 (1985) 12969.
[13] S.E. Ealick, S.A. Rule, D.C. Carter, T.J. Greenhough, B. Sudhakar, W.J. Cook, J. Habash, J.R. Helliwell, J.D. Stoeckler, R.E. Parks, Jr., S.-F. Chen and C.E. Bugg, J. Biol. Chem., 265 (1990) 1812.
[14] A. Bzowska, M. Luic, W. Schroder, D. Shugar, W. Saenger and G. Koellner, FEBS Lett., 367 (1995) 214.
[15] S.E. Ealick, Y.S. Babu, S.W.L. Narayana, W.J. Cook, and C.E. Bugg, in C.E. Bugg and S.E. Ealick (Eds.), Crystallographic and Modeling Methods in Molecular Design, Springer Verlag, New York, 1990, pp. 43–55.
[16] R.R. Copley and G.J. Borton, J. Mol. Biol., 242 (1994) 32.
[17] P. Chakrabarti, J. Mol. Biol., 234 (1993) 463.
[18] Z.F. Kanyo and D.W. Christianson, J. Biol. Chem., 266 (1991) 4264.
[19] S. Halazy, A. Ehrhard, A. Eggenspiller, V. Bergs-Gross and C. Danzin, Tetrahedron, 52 (1996) 177.
[20] S. Halazy, A. Ehrhard and C. Danzin, J. Am. Chem. Soc., 113 (1991) 315.
[21] C.C. Smith, G.F. Wolfe and G.E. Cartwright, in P.L. Altman and D.S. Dittmar (Eds.), Biology Data Book, 2nd edn., Vol. 3, Federation of American Societies for Experimental Biology, Bethesda, MD, 1974, pp. 1751–1754.
[22] T.W. Traut, Mol. Cell. Biochem, 140 (1994) 1.
[23] P.C. Kline and V.L. Schramm, Biochemistry, 32 (1993) 13212.
[24] B.K. Kim, S. Cha and R.E. Parks, Jr., J. Biol. Chem., 243 (1968) 1771.
[25] J.H. Gardner and L.D. Byers, J. Biol. Chem., 252 (1977) 5925.
[26] P.A. Roop and T.W. Traut, J. Biol. Chem., 266 (1991) 7682.
[27] K.F. Jensen, Eur. J. Biochem., 61 (1976) 377.
[28] S. Forsén and S. Linse, Trends Biochem. Sci., 20 (1995) 495.
[29] A. Bzowska, E. Kulikowska and D. Shugar, Z. Naturforsch., Teil C, 45 (1990) 59.
[30] O.H. Lowry, N.J. Rosenberg, A.L. Farr and R.J. Randall, J. Biol. Chem., 193 (1951) 265.
[31] A. Bzowska, unpublished data.
[32] H.M. Kalckar, J. Biol. Chem., 167 (1947) 429.
[33] E. Kulikowska, A. Bzowska, J. Wierzchowski and D. Shugar, Biochim. Biophys. Acta, 874 (1986) 355.
[34] W.P. Schrader, A.R. Stacy and B. Pollara, J. Biol. Chem., 251 (1976) 4026.
[35] P.H. O'Farrel, J. Biol. Chem., 250 (1975) 4007.
[36] C.R. Merril, D. Goldman and M.L. van Keuren, Methods Enzymol., 104 (1984) 441.
[37] P.K. Lehikoinen, M.L. Sinnott and T.A. Krenitsky, Biochem. J., 257 (1989) 355.
[38] R.W. Gilpin and H.L. Sadoff, J. Biol. Chem., 246 (1971) 1475.
[39] B.N. Ames, Methods Enzymol., 8 (1966) 115.
[40] J.R. Lakowicz, Principles of Fluorescence Spectroscopy, Plenum, New York, 1983, pp. 257.
[41] M.R. Eftink and C.A. Ghiron, Anal. Biochem., 114 (1981) 199.
[42] S.S. Lehrer and P.C. Leavis, Methods Enzymol., 49 (1978) 222.
[43] S.S. Lehrer, Biochemistry, 10 (1971) 3254.
[44] G. Scatchard, Ann. New York Acad. Sci., 51 (1949) 660.
[45] B. Kierdaszuk, R. Rigler and S. Eriksson, Biochemistry, 32 (1993) 699.
[46] I.M. Klotz and D.L. Hunston, Biochemistry, 10 (1971) 3065.
[47] K.E. Neet, Methods Enzymol., 64 (1980) 139.
[48] D.V. O'Connor and D. Philips, Time-Correlated Single Photon Counting, Academic Press, London, 1984.
[49] D.J.S. Birch and R.E. Imhof, in J.R. Lakowicz (Ed.), Topics in Fluorescence Spectroscopy, Techniques, Vol. 1, Plenum Press, New York, 1991, pp. 1–95.
[50] J.B.A. Ross, W.R. Laws, K.W. Rousslang and H.R. Wyssbrod, in J.R. Lakowicz (Ed.), Topics in Fluorescence Spectroscopy, Biochemical Applications, Vol. 3, Plenum Press, New York, 1992, pp. 1–63.
[51] B. Kierdaszuk, I. Gryczyński, A. Modrak-Wójcik, A. Bzowska, D. Shugar and J.R. Lakowicz, Photochem. Photobiol., 61 (1995) 319.
[52] C.M. Anderson, S.H. Zucker and T.A. Steitz, Science, 204 (1979) 375.
[53] J.V. Tuttle and T.A. Krenitsky, J. Biol. Chem., 259 (1984) 4065.
[54] T.A. Krenitsky, J.V. Tuttle, W.H. Miller, A.R. Moorman, G.F. Orr and L. Beauchamp, J. Biol. Chem., 265 (1990) 3066.
[55] J.A. Montgomery, Med. Res. Rev., 13 (1993b) 209.
[56] J.L. Kelley, E.W. McLean, R.C. Crouch, D.R. Averett and J.V. Tuttle, J. Med. Chem., 38 (1995) 1005.
[57] S.R. Williams, J.M. Goddard and D.W. Martin, Jr., Nucleic Acids Res., 12 (1984) 5779.